

Electronic properties of EuB_6 in the ferromagnetic regime: Half-metal versus semiconductor

M. Kreissl* and W. Nolting

Lehrstuhl Festkörpertheorie, Institut für Physik, Humboldt-Universität zu Berlin, Newtonstr. 15, 12489 Berlin

To understand the halfmetallic ferromagnet EuB_6 we use the Kondo lattice model for valence and conduction band. By means of a recently developed many-body theory we calculate the electronic properties in the ferromagnetic regime up to the Curie temperature. The decreasing magnetic order induces a transition from halfmetallic to semiconducting behavior along with a band broadening. We show the temperature dependence of the quasiparticle density of states and the quasiparticle dispersion as well as the effective mass, the number of carriers and the plasma frequency which are in good agreement with the experimental data.

PACS numbers: 71.10.-w, 75.50.Pp, 71.30.+h, 75.10.-b, 75.30.-m

I. INTRODUCTION

In the last decade EuB_6 with its interesting and still not fully understood magnetic and electronic properties has attracted considerable interest. For low temperatures it is a ferromagnetic semimetal becoming a paramagnetic semiconductor for higher temperatures. It crystallizes in the cubic CaB_6 structure (spacegroup 221, $\text{Pm}\bar{3}\text{m}$). The divalent Europium ions occupy the corners of the cubic unit cell and at the body centered position sits an octahedron consisting of six Boron atoms. The lattice constant $a=4.19\text{\AA}$ does not change with temperature.¹

EuB_6 exhibits two consecutive phase transitions at $T_C=12.5\text{K}$ and $T_M=15.5\text{K}$.¹ T_C is the bulk Curie temperature. The magnetization follows a Brillouin function and the saturation value is $7\mu_B$ due to the exactly half-filled 4f shell in Europium.³ Nonetheless there are evidences of phase separation above T_C up to 30K ^{2,3}, where bound magnetic polarons⁷ are responsible for the cusplike peak in resistivity and the colossal magnetoresistance at T_M .^{4,5} Concomitant with the bulk magnetic phase transition at T_C is a transition from semimetal to semiconductor.^{6,7}

For low temperatures the semimetallic behavior is proven theoretically and experimentally. Early local density approximation (LDA)⁸ as well as recent band structure calculations in LDA+U⁹ show an overlap of valence and conduction band around the X-point of the Brillouin zone. Shubnikov - de Haas and de Haas - van Alphen measurements^{10,11} agree with that picture as they report electron and hole pockets on the Fermi surface at the X-point. The carrier density is about 0.01 per unit cell for low and 0.001 for higher temperatures.¹² Due to the known lack of correct predictions of band gaps in the LDA the authors in [9] suggest EuB_6 to be halfmetallic in the ferromagnetically ordered phase. That scenario is not ruled out by experiments albeit not proven also.

The resistivity shows a strong peak at T_M and also indicates a metal - insulator transition. Up to T_C and T_M an increase of the carrier concentration, a reduction of the effective mass or a combination of both is responsible for a strong red shift of the plasma frequency.¹³ The

specific electronic properties seem to stem from temperature dependent changes of valence and conduction bands induced by the ferromagnetic alignment of the local moments. The other way around the ferromagnetism is attributed to an RKKY mechanism where the itinerant carriers are responsible for the magnetic exchange. It looks as if the system will be best described by the two band Kondo lattice model introduced in the next section.

Similar models but with focus on other properties of EuB_6 are already studied in a mean-field treatment¹⁴ and in dynamical mean-field theory.¹⁵ The spin polaron model¹⁶ explains the behavior in resistivity and the colossal magnetoresistance effect around T_M . This paper will focus on the range from zero temperature to T_C where the magnetic and metallic phase transitions take place.

II. THEORY

For modeling EuB_6 we will use the Kondo-lattice model,¹⁷ also known as s-f model. The spins of the localized 4f electrons result in a local magnetic moment which interacts with the spin of the itinerant electrons in the valence(v) and conduction(c) band, respectively. The complete two-band Hamiltonian in second quantization is

$$H = \sum_b^{v,c} \sum_{ij\sigma} (T_{ij}^b - \mu\delta_{ij}) a_{bi\sigma}^\dagger a_{bj\sigma} + \sum_{b,b'}^{v,c} J^{bb'} \sum_{j\sigma\sigma'} \frac{1}{2} a_{bj\sigma}^\dagger \tau_{\sigma\sigma'} a_{b'j\sigma'} \mathbf{S}_j. \quad (1)$$

The first term in (1) describes the kinetic part of the electrons in band b with the hopping integrals T_{ij}^b between two lattice sites \mathbf{R}_i and \mathbf{R}_j that are connected to the wave vector \mathbf{k} dependent Bloch energies $\varepsilon_{\mathbf{k}}^b$ via Fourier transformation $T_{ij}^b = \frac{1}{N} \sum_{\mathbf{k}} \varepsilon_{\mathbf{k}}^b e^{i\mathbf{k}\mathbf{R}_{ij}}$. The chemical potential is μ and $a_{bj\sigma}^\dagger$ ($a_{bj\sigma}$) the creation (annihilation) operator of an electron with spin σ at lattice site \mathbf{R}_j in band b.

The second term in (1) describes the s-f interaction between the itinerant band electrons and the local moments \mathbf{S}_j . $\tau_{\sigma\sigma'}$ are the Pauli matrices and $J^{bb'}$ the coupling constants. In contrast to the kinetic part the interaction term does not need to be diagonal in band indices. It might be possible that during the s-f interaction the itinerant electron in band b hops to the other band b'. That possibility is included in (1).

In EuB_6 the valence band is formed from Boron 2p and Europium 4f states and the conduction band from Boron 2p and Europium 5d states which overlap at the X-point⁹. The possible interband transitions are negligible by symmetry reasons.

Therefore we will set $J^{bb'}$ diagonal, resulting in the following Hamiltonian

$$H = \sum_b^{v,c} (H_s^b + H_{sf}^b). \quad (2)$$

H_s^b is the kinetic term for band b

$$H_s^b = \sum_{ij\sigma} (T_{ij}^b - \mu\delta_{ij}) a_{bi\sigma}^\dagger a_{bj\sigma}. \quad (3)$$

H_{sf}^b describes the s-f interaction for band b

$$H_{sf}^b = -\frac{1}{2} J^b \sum_{j\sigma} (z_\sigma S_j^z n_{bj\sigma} + S_j^\sigma a_{bj-\sigma}^\dagger a_{bj\sigma}) \quad (4)$$

where we used $n_{bj\sigma} = a_{bj\sigma}^\dagger a_{bj\sigma}$, $z_\sigma = \delta_{\sigma\uparrow} - \delta_{\sigma\downarrow}$ and $S_j^\sigma = S_j^x + iz_\sigma S_j^y$. The first term in (4) describes an Ising-like interaction and the second the spin-flip processes.

The coupling constant J^b is positive (ferromagnetic alignment) for the conduction band electrons and negative (anti-ferromagnetic alignment) for the valence band electrons⁹. We assume the same magnitude J for both bands, hence $J^v = -J$ and $J^c = J$.

It goes without saying, that the k-independent coupling constant is an oversimplification. However, this is unavoidable due to mathematical difficulties.

A. Green Function

We are mainly interested in the single electron Green function

$$\begin{aligned} G_{\mathbf{k}\sigma}^b(E) &= \langle\langle a_{b\mathbf{k}\sigma}; a_{b\mathbf{k}\sigma}^\dagger \rangle\rangle \\ &= \frac{1}{N} \sum_{ij} \langle\langle a_{bi\sigma}; a_{bj\sigma}^\dagger \rangle\rangle e^{i\mathbf{k}\mathbf{R}_{ij}} \end{aligned} \quad (5)$$

from which all electronic properties can be calculated. The operator $a_{b\mathbf{k}\sigma}^\dagger$ ($a_{b\mathbf{k}\sigma}$) is the creation (annihilation) operator in k-space. To derive the Green function we solve the equation of motion

$$E G_{\mathbf{k}\sigma}^b(E) = \hbar + \langle\langle [a_{b\mathbf{k}\sigma}, H_s^b + H_{sf}^b]_-; a_{b\mathbf{k}\sigma}^\dagger \rangle\rangle. \quad (7)$$

For some special cases the equation of motion can be solved exactly but for most of the cases one needs to apply specific approximations for the higher Green functions to decouple. Decoupling means it is possible to introduce a self energy $\Sigma_{\mathbf{k}\sigma}^b(E)$ which formally solves

$$\langle\langle [a_{b\mathbf{k}\sigma}, H_{sf}^b]_-; a_{b\mathbf{k}\sigma}^\dagger \rangle\rangle_E = \Sigma_{\mathbf{k}\sigma}^b(E) G_{\mathbf{k}\sigma}^b(E) \quad (8)$$

and thus the Green function reads

$$G_{\mathbf{k}\sigma}^b(E) = \frac{\hbar}{E - \varepsilon_{\mathbf{k}}^b + \mu - \Sigma_{\mathbf{k}\sigma}^b(E)}. \quad (9)$$

B. Self Energy

In this section we will introduce an appropriate approximation of the self energy for the almost empty conduction band, which is ferromagnetically coupled to the local magnetic moments, and the almost filled valence band which is anti-ferromagnetically coupled.

For the **conduction band** it is possible to apply the interpolation formula for the self-energy given in [20] which is valid for low densities ($e \rightarrow 0$) and covers the following exactly solvable special cases:

- Zero-bandwidth limit ($\varepsilon_{\mathbf{k}} \rightarrow T_0$)
- Ferromagnetically saturated semiconductor ($\langle S^z \rangle = S$, $e=0$)
- Second order perturbation theory in J
- High energy expansion

The resulting self-energy is

$$\begin{aligned} \Sigma_\sigma^c &= \Sigma_\sigma^{e \rightarrow 0}(E) = \\ &= -\frac{1}{2} J^c \left(M_\sigma - \frac{1}{2} J^c \frac{a_\sigma G_0(E - \frac{1}{2} J^c M_\sigma)}{1 - \frac{1}{2} J^c G_0(E - \frac{1}{2} J^c M_\sigma)} \right) \end{aligned} \quad (10)$$

where $M_\sigma = z_\sigma \langle S^z \rangle$, $a_\sigma = S(S+1) - m_\sigma(m_\sigma+1)$ and $G_0(E) = \frac{1}{N} \sum_{\mathbf{k}} \frac{\hbar}{E - \varepsilon_{\mathbf{k}} + \mu}$ is the free propagator. The magnetization $\langle S^z \rangle$ will be calculated via the Brillouin function which is in agreement with the measurements in [3].

Since the **valence band** is almost completely filled, let us change for one moment from the electronic picture to a hole like quasiparticle picture. Such a hole corresponds to a missing electron in an otherwise completely filled valence band. To keep the negative coupling constant for the electrons in the valence band, the coupling constant for the holes must have opposite sign ($J^v(e) \rightarrow -J^v(h)$). The self energy for the holes in the low density approximation ($h \rightarrow 0$) from [20] then reads

$$\begin{aligned} \Sigma_\sigma^{h \rightarrow 0}(E) &= \\ &= \frac{1}{2} J^v \left(M_\sigma + \frac{1}{2} J^v \frac{a_\sigma G_0(E + \frac{1}{2} J^v M_\sigma)}{1 + \frac{1}{2} J^v G_0(E + \frac{1}{2} J^v M_\sigma)} \right). \end{aligned} \quad (11)$$

Returning to the electron picture through reversing the spin ($M_\sigma(h) \rightarrow -M_\sigma(e)$), the self energy for the electrons in the almost completely filled valence band then is

$$\Sigma_\sigma^v(E) = \Sigma_{-\sigma}^{h \rightarrow 0}(E) = -\frac{1}{2}J^v \left(M_\sigma - \frac{1}{2}J^v \frac{a_{-\sigma}G_0(E - \frac{1}{2}J^v M_\sigma)}{1 + \frac{1}{2}J^v G_0(E - \frac{1}{2}J^v M_\sigma)} \right). \quad (12)$$

In fact this self-energy covers the above mentioned special cases for full bands.

Now we can put the selfenergies for both bands, (10) and (12) in (9) and calculate the Greenfunction.

III. RESULTS

As described in the previous section we are able to calculate the one electron Green function with the given self energies for both bands. In this section our results are presented. The band index will be skipped as it should be clear that the following calculations are formal equivalent for both bands.

Several free parameters need to be adapted. The spin is $S=\frac{7}{2}$ due to the exactly half filled 4f shell of Europium and the coupling constant $J=0.2\text{eV}$ is in accordance with current literature. We assume a modified tight binding dispersion $\varepsilon_{\mathbf{k}}$ for simple cubic¹⁸ with the band gap located at the X-point instead of Γ .

$$\varepsilon_{\mathbf{k}} = T_0 - \frac{W}{6} \left(\cos(k_x a - \pi) + \cos(k_y a) + \cos(k_z a) \right) \quad (13)$$

Here T_0 is the band's center of gravity and W the bandwidth. The widths of the tight binding bands are crucial for our model calculation since the effective coupling strength is $\frac{JS}{W}$. The mean values of the anisotropic effective masses m^* given in [9] are $1.2m_e$ and $0.35m_e$ for valence and conduction band, respectively. From that we can calculate the corresponding bandwidths

$$W = \frac{6\hbar^2}{m^*a^2} \quad (14)$$

which leads to $W^v=2.2\text{eV}$ and $W^c=7.4\text{eV}$ and is in agreement with the approximated widths from the band structure calculations for the hexaborides^{8,9}. In accordance with the measured band gap for the non-magnetic ($J=0$) CaB_6 in [21] we assume an intrinsic gap of $\Delta=0.25\text{eV}$. The chemical potential is determined to result in compensated electrons and holes since the intrinsic band structure is semiconducting.

A. Q-DOS

Figure 1 shows the quasiparticle density of states (Q-DOS) for the electrons in the valence and conduction band at different temperatures (0K , $\frac{3}{4}T_C$, T_C)

$$\varrho_\sigma(E) = -\frac{1}{N\hbar} \sum_{\mathbf{k}} \frac{1}{\pi} \text{Im} G_{\mathbf{k}\sigma}(E - \mu). \quad (15)$$

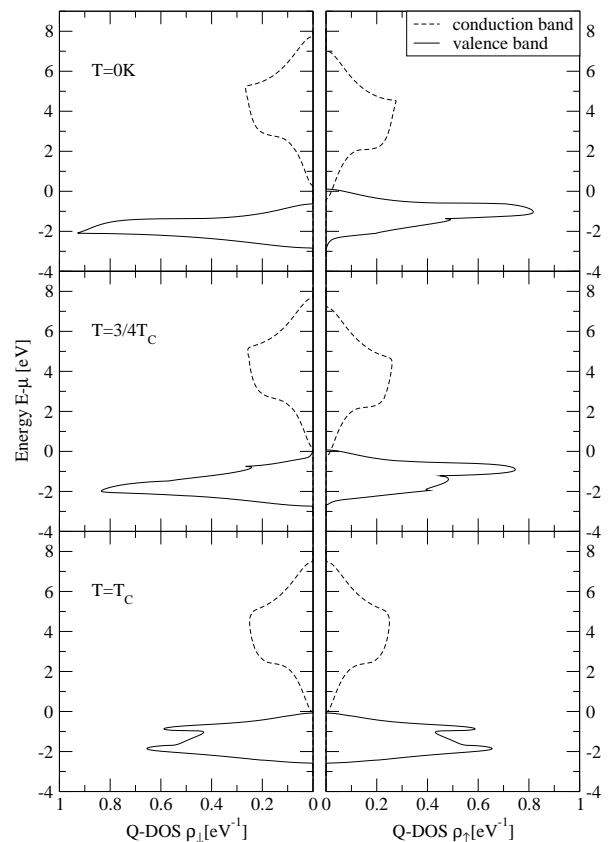


FIG. 1: Quasiparticle density of states for spin down (left) and up (right) electrons in valence (straight line) and conduction band (dashed line) at $T=0\text{K}$ (top), $\frac{3}{4}T_C$ (middle) and T_C (bottom), $S=3.5\text{eV}$, $J=0.2\text{eV}$, $W^v=2.2\text{eV}$, $W^c=7.4\text{eV}$, $\Delta=0.25\text{eV}$.

Since $JS \ll W$ we are in the weak coupling regime, although the effective coupling strength $\frac{JS}{W}$ is different for conduction and valence band which leads to different results.

For the **conduction band** the Q-DOS is shifted with magnetization in a mean-field like manner by $\frac{1}{2}JM_\sigma$. Even so one can see an overall band broadening with decreasing magnetization.

For the **valence band** some correlation effects are visible. At $T=0\text{K}$ the spin down band is rigidly shifted by $\frac{1}{2}JS$. Since the local moments are completely aligned no spin exchange is possible for spin down electrons (keep the anti-ferromagnetic coupling in mind) hence there is no deformation of that band. In the spin up channel one sees a dip between two overlapping subbands. The lower subband describes electrons which flip their spin during the interaction with the local spin system, emitting a magnon. Thus their lifetime is decreased. The upper subband is connected to a stable quasiparticle known as magnetic polaron which propagates through the lattice dressed by a virtual cloud of magnons (for more details see [20]).

At higher temperatures the scattering for both spin

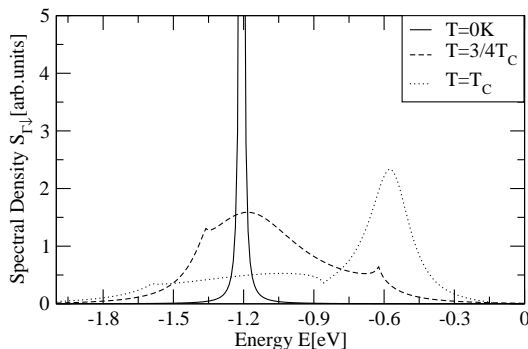


FIG. 2: Quasiparticle spectral density at the Γ -point for spin down quasiparticles in the valence band at $T=0\text{K}$, $\frac{3}{4}T_C$ and T_C , $S=3.5\text{eV}$, $J=0.2\text{eV}$, $W^v=2.2\text{eV}$, $W^c=7.4\text{eV}$, $\Delta=0.25\text{eV}$

orientations becomes more likely, explaining the deformation of the Q-DOS in both spin channels. With decreasing magnetization (increasing temperature) the difference between the up and down spectrum decreases and vanishes at T_C due to the missing alignment of the local moments.

What is also shown in figure 1 is a transition from halfmetallic to semiconducting behavior undergoing the magnetic phase transition. The overlap of the spin up bands at 0K is 0.5eV and the gap between valence and conduction band at T_C is 0.04eV . The band gap at T_C is in accordance with tunnel experiments⁶.

With a mean-field treatment of the Hamiltonian one could also show the halfmetal to semiconductor transition. The tight binding dispersion would be shifted rigidly by $\frac{1}{2}JM_\sigma$, resulting in an overlap at $T=0\text{K}$ of 0.45eV for spin up and the band gap at T_C of 0.25eV . The smaller band gap within our approach results from the interaction between the electrons and the local moments even above T_C . Although the net magnetization at T_C is zero, the statistically distributed magnetic moments influence the electronic structure which results in the band broadening. In a meanfield treatment the interaction is simply switched off at T_C .

B. Spectral Density

The spectral density

$$S_{\mathbf{k}\sigma}(E) = -\frac{1}{\pi} \text{Im} G_{\mathbf{k}\sigma}(E) \quad (16)$$

can be compared directly with angle and spin resolved (inverse) photo emission experiments.

Figure 2 shows the spectral density at $\Gamma=(0,0,0)$ for a spin down quasiparticle in the valence band at different temperatures. As explained in the previous section, at zero temperature the spin down electron in the valence band cannot exchange its spin with the local moments because they are fully aligned. Thus the quasiparticle has infinite lifetime. That fact is visualized in figure

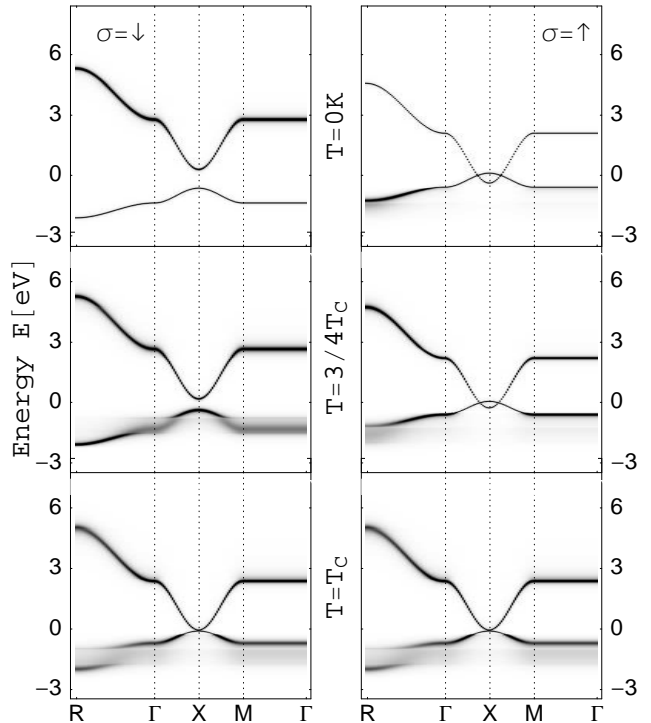


FIG. 3: Spectral density as grayscale at k-points along the irreducible Brillouin Zone for spin down (left) and up (right) quasiparticles at 0K (top), $\frac{3}{4}T_C$ (middle) and T_C (bottom), $S=3.5\text{eV}$, $J=0.2\text{eV}$, $W^v=2.2\text{eV}$, $W^c=7.4\text{eV}$, $\Delta=0.25\text{eV}$

2 as a sharp peak for $T=0\text{K}$. For higher temperatures and less magnetic ordering, magnons are excited and can be absorbed by the spin down electron in the valence band. Therefore the lifetime is decreased with temperature which is represented by the wide peaks in figure 2.

That evaluation of the spectral density could be done for every k-point. In figure 3 we show the spectral density as grayscale along the standard symmetry points in the Brillouin Zone, which makes a temperature dependent band structure.

The same effects we noticed in the Q-DOS (Fig. 1) can be seen in the density plots (Fig. 3). The spin up conduction band and spin down valence band is undeformed and rigidly shifted, represented by the thin lines. The smearing occurs where spin flip scattering is possible.

For example in the plot for spin up quasiparticles in the valence band at $T=0\text{K}$ (fig. 3, top right, lower band) we can distinguish between an undeformed, sharp region around the X-point and a blurred region. These are connected to the two subbands mentioned in the previous section. The lower one describes quasiparticles that are involved in spin flip scattering, their lifetime is decreased. Whereas for quasiparticles in the upper subband no real spin flip processes are possible because there are no states

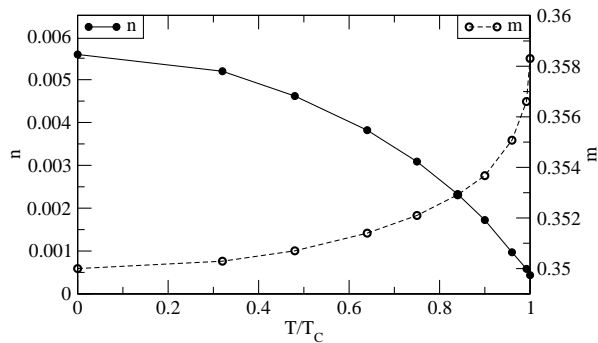


FIG. 4: Temperature dependence of the effective mass m (dashed line) and occupation number n (straight line) of spin up quasiparticles in the conduction band, $S=3.5\text{eV}$, $J=0.2\text{eV}$, $W^v = 2.2\text{eV}$, $W^c = 7.4\text{eV}$, $\Delta=0.25\text{eV}$.

in the corresponding spin down region. Their lifetime is infinite.

At higher temperatures the spin flip processes are possible for spin up and down. It occurs especially in the flat regions of the dispersion where the possibility of scattering is enhanced due to the smaller velocity.

Along the $\Gamma - R$ direction occurs a band splitting approaching T_C . In a photo emission experiment it would be difficult to resolve the light shaded regions in figure 2 because of the short lifetime of the quasiparticles. Therefore one might wonder about two bands coming from Γ and R which do not fit together. They can be explained with our many-body theory of the interaction between the electrons and the local moments.

The effects in the conduction band are less pronounced due to the weaker effective coupling. Nevertheless one can see that the lines get smeared with temperature due to the interaction.

C. Plasma Frequency

Now we will show the qualitative behavior of the effective mass, occupation number and plasma frequency. That can be compared directly with the experiments and will be a measure whether our Kondo lattice model is able to explain some of the properties of EuB_6 .

Via the partial derivative of the real part of the self energy R_σ with respect to the resonance energies $E_{\mathbf{k}\sigma} = \varepsilon_{\mathbf{k}} - \mu + R_\sigma(E_{\mathbf{k}\sigma})$ it is possible to derive the effective mass of the quasi-particles

$$m_{\mathbf{k}\sigma}(T) = 1 - \left(\frac{\partial R_\sigma(T, E_{\mathbf{k}\sigma})}{\partial E_{\mathbf{k}\sigma}(T)} \right)_{\varepsilon_{\mathbf{k}}} \quad (17)$$

The effective mass at the X-point for a spin up quasiparticle in the conduction band is shown in figure 4 (dashed line). One can see a slight increase with increasing temperature. That is in qualitative agreement with the experimental results in [13] and [12].

The occupation number can be computed by

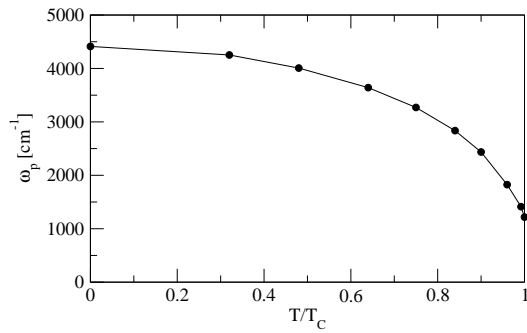


FIG. 5: Temperature dependence of the plasma frequency for the conduction band.

$$n_\sigma(T) = \sum_{\mathbf{k}} \langle a_{\mathbf{k}\sigma}^\dagger a_{\mathbf{k}\sigma} \rangle(T) \quad (18)$$

$$= \int f_-(T, E) \rho_\sigma(T, E) dE \quad (19)$$

where $f_-(T, E) = (1 + \exp(\frac{E - \mu}{k_B T}))^{-1}$ is the Fermi function (k_B is the Boltzmann constant).

Figure 4 (straight line) shows the occupation number for spin up quasi-particles versus temperature. In the previous section the decreasing band overlap with temperature due to the reduced magnetization was introduced. This is why the occupation number decreases dramatically by an order of magnitude. This agrees with the Hall data in [12].

Figure 5 shows the calculated plasma frequency versus temperature

$$\omega_p(T) = \sqrt{\frac{e^2 n(T)}{\epsilon_0 m(T)}} \quad (20)$$

with the electric charge e and the dielectric constant ϵ_0 . The reduction of free carriers and the increasing effective mass with increasing temperature lead to a red shift of the plasma frequency. That is in excellent agreement with magneto optical results in [13].

D. Half metallicity

As already mentioned we derive half metallic behavior in the whole ferromagnetic regime. To clarify that, figure 6 shows the shrinking band overlap for spin up (straight line) and the gap for spin down quasiparticles (dashed line) versus temperature. At zero temperature the spin up bands overlap by 0.5eV and the spin down bands are separated by 0.9eV . With decreasing magnetization the spin up and down bands are shifted and merge at the Curie temperature, resulting in a band gap of 0.04eV at T_C .

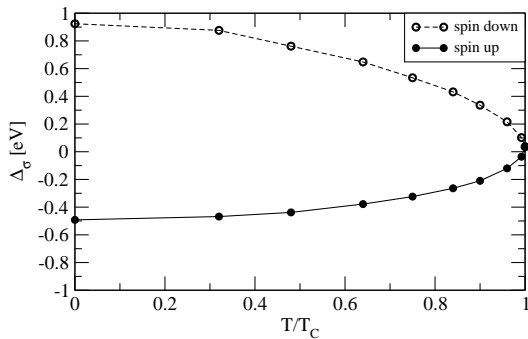


FIG. 6: Relative temperature dependence of the band overlap (straight line) for spin up and the band gap (dashed line) for spin down quasiparticles.

IV. CONCLUSIONS

Starting from the two band Kondo lattice Hamiltonian with opposite sign of the coupling constants for valence and conduction band electrons we were able to reproduce the metal-insulator transition for EuB_6 concomitant with the magnetic phase transition. The synchronous band broadening is verified through our model, too. The experimentally measured dependence of effective mass, oc-

cupation number and plasma frequency are qualitatively confirmed.

In our model the change in the carrier concentration dominates over the change of the effective mass, whereas in the model proposed by Hirsch²⁴ only the change of the effective mass is made responsible for the specific properties of EuB_6 .

With the chosen parameters, motivated by experiments, EuB_6 turns out to be not only metallic but halfmetallic in the ferromagnetic regime. That would need further experimental investigations since the halfmetallic behavior is announced as a possible result of future GW-calculations in [9] and not explicitly excluded in the Shubnikov - de Haas and de Haas - van Alphen measurements.

A possible refinement of our calculation will be to consider a real band structure for EuB_6 . Above T_C up to 30K is a regime of phase separation where bound magnetic polarons and percolation effects play a significant role. That is not included in our model yet, since the magnetization is not calculated self consistently. That should be done in future corresponding to [22]. Further on it would be interesting to study the diluted system $\text{Ca}_x\text{Eu}_{1-x}\text{B}_6$ as was done in [23].

* Electronic address: kreissl@physik.hu-berlin.de

- ¹ S. Sullow, I. Prasad, M. C. Aronson, J. L. Sarrao, Z. Fisk, D. Hristova, A. H. Lacerda, M. F. Hundley, A. Vigliante, and D. Gibbs, *Phys. Rev. B* **57**, 5860 (1998)
- ² S. Sullow, I. Prasad, M.C. Aronson, S. Bogdanovich, J.L. Sarrao, and Z. Fisk, *Phys. Rev. B* **62**, 11626 (2000)
- ³ W. Henggeler, H.R. Ott, D.P. Young, and Z. Fisk, *Solid State Commun.* **108**, 929 (1998)
- ⁴ R. R. Urbano, P. G. Pagliuso, C. Rettori, S. B. Oseroff, J. L. Sarrao, P. Schlottmann, and Z. Fisk, *Phys. Rev. B* **70**, 140401(R) (2004)
- ⁵ M. L. Brooks, T. Lancaster, S. J. Blundell, W. Hayes, F. L. Pratt, and Z. Fisk, *Phys. Rev. B* **70**, 020401(R) (2004)
- ⁶ B. Amsler, Z. Fisk, J. L. Sarrao, S. von Molnar, M. W. Meisel, and F. Sharifi, *Phys. Rev. B* **57**, 8747 (1998)
- ⁷ P. Nyhus, S. Yoon, M. Kauffman, S. L. Cooper, Z. Fisk, and J. Sarrao, *Phys. Rev. B* **56**, 2717 (1997)
- ⁸ S. Massidda, A. Continenza, T. M. Pascale, and R. Monnier, *Z. Phys. B* **102**, 83 (1997)
- ⁹ J. Kunes and W. E. Pickett, *Phys. Rev. B* **69**, 165111 (2004)
- ¹⁰ M. C. Aronson, J. L. Sarrao, Z. Fisk, M. Whitton, and B. L. Brandt, *Phys. Rev. B* **59**, 4720 (1999)
- ¹¹ R. G. Goodrich, N. Harrison, J. J. Vuillemin, A. Teklu, D. W. Hall, Z. Fisk, D. Young, and J. Sarrao, *Phys. Rev. B* **58**, 14896 (1998)
- ¹² S. Paschen, D. Pushin, M. Schlatter, P. Vonlanthen, H.

- R. Ott, D. P. Young, and Z. Fisk, *Phys. Rev. B* **61**, 4174 (2000)
- ¹³ L. Degiorgi, E. Felder, H.R. Ott, J.L. Sarrao, and Z. Fisk, *Phys. Rev. Lett.* **79**, 5134 (1997)
- ¹⁴ I.Y. Korenblit, *Phys. Rev. B* **64**, 100405(R) (2001)
- ¹⁵ Chungwei Lin and Andrew J. Millis, *Phys. Rev. B* **71**, 075111 (2005)
- ¹⁶ J. Chatterjee, U. Yu, and B. I. Min, *Phys. Rev. B* **69**, 134423 (2004).
- ¹⁷ W. Nolting, *Phys. Status Solidi B* **96**, 11 (1979)
- ¹⁸ R. J. Jelitto, *J. Phys. Chem. Solids* **30**, 609 (1969)
- ¹⁹ J. D. Denlinger, J. A. Clack, J. W. Allen, G.-H. Gweon, D. M. Poirier, C. G. Olson, J. L. Sarrao, A. D. Bianchi, and Z. Fisk, *Phys. Rev. Lett.* **89**, 157601 (2002)
- ²⁰ W. Nolting, G. G. Reddy, A. Ramakanth, and D. Meyer, *Phys. Rev. B* **64**, 155109 (2001)
- ²¹ Jung-Ho Kim, Youngwoo Lee, C. C. Homes, Jong-Soo Rhyee, B. K. Cho, S.-J. Oh, and E. J. Choi, *Phys. Rev. B* **71**, 075105 (2005)
- ²² C. Santos, W. Nolting, V. Eyert, *Phys. Rev. B* **69**, 214412 (2004)
- ²³ Vitor M. Pereira, J. M. B. Lopes dos Santos, Eduardo V. Castro, and A. H. Castro-Neto, *Phys. Rev. Lett.* **93**, 147202 (2004)
- ²⁴ J.E. Hirsch, *Phys. Rev. B* **59**, 436 (1999)